Journal of Magnetic Resonance 253 (2015) 91–97

Contents lists available at ScienceDirect

Journal of Magnetic Resonance

journal homepage: www.elsevier.com/locate/jmr

Bottom-up and top-down solid-state NMR approaches for bacterial biofilm matrix composition

Lynette Cegelski

Department of Chemistry, Stanford University, CA 94305, United States

ARTICLE INFO

Article history:
Received 19 November 2014
Revised 7 January 2015

Keywords:
Bacterial biofilms
Extracellular matrix
Solid-state NMR
CPMAS
REDOR
E. coli
V. cholerae

ABSTRACT

The genomics and proteomics revolutions have been enormously successful in providing crucial "parts lists" for biological systems. Yet, formidable challenges exist in generating complete descriptions of how the parts function and assemble into macromolecular complexes and whole-cell assemblies. Bacterial biofilms are complex multicellular bacterial communities protected by a slime-like extracellular matrix that confers protection to environmental stress and enhances resistance to antibiotics and host defenses. As a non-crystalline, insoluble, heterogeneous assembly, the biofilm extracellular matrix poses a challenge to compositional analysis by conventional methods. In this perspective, bottom-up and top-down solid-state NMR approaches are described for defining chemical composition in complex macrosystems. The "sum-of-the-parts" bottom-up approach was introduced to examine the amyloid-integrated biofilms formed by *Escherichia coli* and permitted the first determination of the composition of the intact extracellular matrix from a bacterial biofilm. An alternative top-down approach was developed to define composition in *Vibrio cholerae* biofilms and relied on an extensive panel of NMR measurements to tease out specific carbon pools from a single sample of the intact extracellular matrix. These two approaches are widely applicable to other heterogeneous assemblies. For bacterial biofilms, quantitative parameters of matrix composition are needed to understand how biofilms are assembled, to improve the development of biofilm inhibitors, and to dissect inhibitor modes of action. Solid-state NMR approaches will also be invaluable in obtaining parameters of matrix architecture.

1. Introduction

> *"When once we know what the molecular architecture of the proteins and other large molecules that carry the physiological activity of the human body is, what the relation of the structure of these molecules is to that of the vectors of disease, and of the drugs, such as penicillin and the sulfa drugs, that serve effectively in protecting us against infectious disease, what changes in molecular architecture are associated with the degenerative diseases – then we can attack the problem of the degenerative diseases in an effective way, using the methods of attack that are suggested by this knowledge."*
> [Linus Pauling. From the lecture "Molecular Architecture and the Processes of Life," Nottingham, England, 1948.]

It was only three years before Pauling delivered the lecture from which the above text is quoted when the first NMR results were reported by Bloch et al. studying a liquid (H_2O) [1] and Purcell et al. examining a solid (paraffin) [2]. Bloch and Purcell went on to share the Nobel Prize in Physics in 1952. The first protein crystal structures, of myoglobin [3] and hemoglobin [4], were reported in 1960. Throughout the subsequent fifty years, science made revolutionary strides to reveal the molecular architecture of life's most fundamental building blocks and machines. New details, new structures, and new discoveries continue to emerge and expand our understanding of life systems. Indeed, the genomics and proteomics revolutions have been enormously successful in generating full genome sequences for an increasing number of organisms and in predicting and determining the structures of a steadily increasing number of proteins. In essence, these data provide crucial "parts lists" for biological systems. Yet, formidable challenges exist in generating complete descriptions of how the parts function and assemble into macromolecular complexes and whole-cell assemblies. Through old and new and emerging cutting-edge technologies across disciplines, experimental and computational experiments are rapidly being developed and implemented in order to address such outstanding problems that will improve our understanding of biological assembly processes and function. Solid-state NMR spectroscopy has proven to be a powerful ally in generating more complete descriptions of macromolecular assemblies. Indeed, solid-state NMR has a rich history as

E-mail address: cegelski@stanford.edu

http://dx.doi.org/10.1016/j.jmr.2015.01.014
1090-7807/

an analytical tool to study the composition, structure, dynamics, and function of solid materials, ranging from coal and earth materials, industrial polymers and catalysts to biomaterials including spider silk, insect exoskeletons, amyloids, membrane proteins, cell walls, whole cells and intact tissues.

Bacterial biofilms are complex multicellular bacterial communities protected by a slime-like extracellular matrix that confers protection to environmental stress such as desiccation and shear flow and enhances bacterial resistance to antibiotics and host defenses [5–8]. The determination of extracellular matrix composition and architecture is crucial to understanding biofilm function and to developing strategies to inhibit matrix assembly and biofilm formation [9]. Genetic and molecular assays together with high-resolution microscopy have provided crucial information regarding factors that help to regulate biofilm formation and molecular factors such as specific proteins and polysaccharides that participate in matrix production [10]. Metabolomic NMR methods have also provided insights to survey and compare the changes in cellular signals and components associated with the cellular transition to the biofilm lifestyle [11], and elegant imaging mass spectrometry approaches have been employed to locate the presence of specific matrix components surrounding cells in the context of intact biofilms [12,13]. Yet, these various approaches are not well suited to providing a total accounting of matrix composition and outstanding questions remain regarding the overall balance of protein *vs* polysaccharides *vs* other components in biofilms formed by diverse microorganisms [14]. The approximation of protein and polysaccharide concentrations, for example, have relied on protocols that attempt to solubilize matrix material and quantify the parts, either through soluble-based assays in the case of proteins or through selective precipitation protocols using various organic solvents to attempt to precipitate polysaccharides separately from other biofilm parts [10,15]. However, many biofilms are recalcitrant to complete dissolution and quantification in these assays and solvent based extractions and precipitations often contain additional non-targeted components that contribute to the sample mass. These considerations compromise estimates of protein and polysaccharide composition. We have found, for example, that a standard BCA (bicinchoninic acid) protein assay can severely underestimate protein content in ECM material. As one of several available protein assays, the BCA assay relies on the ability of proteins to reduce Cu^{2+} ions with colorimetric detection of Cu^{1+} by bicinchoninic acid, forming a purple colored product. The success of this assay can be compromised by the inaccessibility of protein peptide bonds within a dense matrix with extensive interactions with other components or due to competitive complexation of Cu^{2+} by other components in a complex sample. Harsh degradative methods can also lead to undesired perturbations of the material. Bacterial biofilms and extracellular matrix material have, on the other hand, been examined extensively by Fourier transform infrared spectroscopy to generally profile the types of chemical functionalities present in intact samples and particularly to permit comparisons across samples, assigning spectral signatures to carbonyls, peptide bonds, aromatics and aliphatics, for example, but have not permitted a complete accounting of biofilm composition [16]. A solid-state NMR study of the extracted ECM from biofilms growing on acid mine drainage also monitored the change in polysaccharide chemical shifts between two samples to qualitatively compare two biofilms and avoided the degradative measures associated with solution-based assays [17].

We recently reported the first determination of the molecular composition of the intact extracellular matrix of a bacterial biofilm [18]. This review will focus on the advances we have made in using solid-state NMR with complementary microscopy and biochemical techniques to define and characterize the composition of the extracellular matrix of bacterial biofilms, describing two different NMR approaches that are widely applicable to other organisms and macromolecular systems. In the case of *Escherichia coli*, we implemented a "sum-of-the-parts" bottom-up approach [18] and in the case of *Vibrio cholerae* we developed a top-down NMR approach [19]. In both methods, protocols were optimized to ensure non-perturbative preparation of matrix material from each organism and samples were examined extensively by biochemical characterization and microscopy. The integrated approach is crucial to defining the nature of the material being studied, ensuring that that most appropriate samples are being examined by NMR, and ultimately to ensuring the biological relevance of the NMR discoveries that drive our evolving understanding of bacterial biofilm composition, structure, and function.

2. Extracellular matrix composition of curli-integrated *E. coli* agar biofilms: a bottom-up NMR approach

2.1. Curli-integrated biofilm formation

The author's interest in *E. coli* biofilms stemmed from her fascination with *E. coli*'s production of functional amyloid fibers termed curli and her discovery of small-molecule inhibitors that interfered with curli assembly *in vivo* and *in vitro* and prevented biofilm formation [20]. This fascination extends to questions surrounding the assembly of these fibers, how they mediate adhesion and contribute to the formation and stability of biofilms, and their potential contribution to the pathogenesis of uropathogenic *E. coli* during urinary tract infection [21,22]. Furthermore, the general production of bacterial amyloid fibers by microbes in the human GI tract, bladder, or other niche could have implications for providing possible amyloid seeds that could influence amyloid assembly processes of human proteins associated with amyloid-related diseases.

Curli were first identified as adhesive fimbriae in 1989 by Normark and coworkers [23] and later identified as being amyloid fibers in 2002 by Chapman, Hultgren, and coworkers [24]. Even before their identification as amyloid, curli were well-studied for their contributions to biofilm formation in *E. coli* and Salmonella species, particularly for agar-grown biofilms [25,26]. Cegelski and coworkers also identified curli as being required for biofilm formation at the air–liquid interface (biofilms termed "pellicles") [20] and have more recently examined the mechanical properties and molecular determinants associated with bacterial pellicles [27–30]. Cellulose is another major component that has been extensively studied for its role in biofilm formation in *E. coli* and Salmonella [26,31], yet determinations of the amounts of curli, cellulose, and possibly other components in the biofilm were not available prior to our work described below.

2.2. Matrix isolation surprise and considerations

In implementing and optimizing protocols to isolate extracellular matrix material from biofilms, which include the cells plus the matrix material, we discovered that we could isolate mechanically robust supramolecular structures that surround *E. coli* like cocoons or baskets in amyloid-integrated bacterial biofilms [18] (Fig. 1). These baskets are able to maintain their shape upon separation from bacteria through the shear forces exerted during use of a tissue homogenizer. The simple homogenization is gentle enough to not lyse *E. coli* cells and is sufficient to remove much of the matrix material surrounding *E. coli*. One can also perform such matrix extractions on the smaller scale, using 1.5 mL microcentrifuge tubes and vortexing, and observe the intact basket-like structures (Fig. 1). In addition to the basket-like structures, one also observes similar matrix material without the definitive shape of baskets that

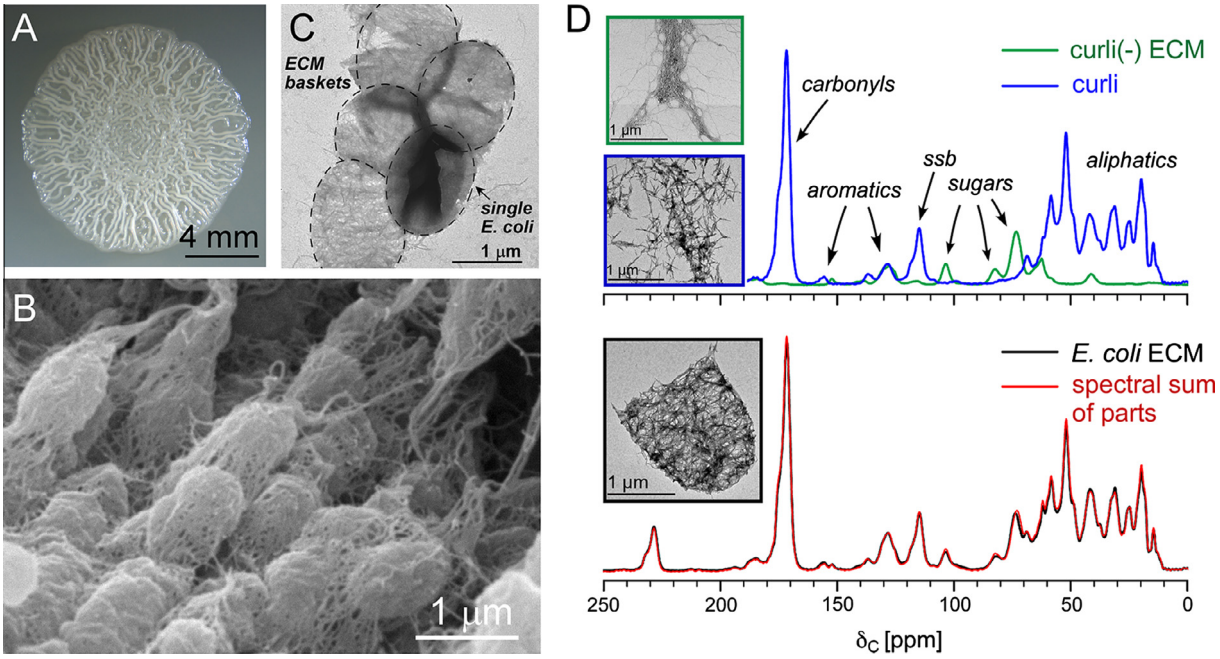

Fig. 1. The bottom-up approach: *E. coli* biofilm phenotypes and ECM composition by solid-state NMR. (A) The hallmark wrinkled colony morphology associated with biofilm formation of *E. coli* growing on YESCA nutrient agar. (B) Scanning electron micrograph on biofilms formed by the same uropathogenic *E. coli* strain, UTI89, as in panel A. (C) Transmission electron micrograph of a collection of ECM baskets following disruption of the biofilm with the tissue homogenizer, prior to low-speed centrifugation to remove intact cells (one bacterium present in TEM image). (D) The spectral sum of the UTI89Δ*csgA* extracellular material and purified curli (top) completely recapitulates the ^{13}C CPMAS spectrum of the intact UTI89 ECM (bottom), each associated with transmission electron micrographs associated with the samples. MAS was performed at 7143 Hz, and 32,768 scans were obtained for each spectrum. This figure is adapted from Ref. [18].

could have been matrix material connecting cells to one another and from baskets that were sheared apart, losing their three-dimensional shape. In preparing samples for NMR analysis, we observed that some flagella were present in the preparations. This was detected by electron microscopy and annotated by protein gel electrophoresis and mass spec protein identification [18]. Protein gels showed the major flagellar protein, FliC, as the only major protein other than the curli subunit, CsgA. Flagella are not required for *E. coli* biofilm formation on agar and do not contribute to the insoluble structural matrix material as evidenced by electron microscopy, so flagella were removed through SDS treatment to prepare samples for the primary NMR analysis.

2.3. Sum-of-the-parts

Together with EM and biochemical analyses, we provided a complete "sum-of-the-parts" accounting of the insoluble matrix using solid-state NMR [18]. In this bottom-up approach, we obtained ^{13}C CPMAS spectra of: (i) purified curli; (ii) the curli-free ECM produced by the curli mutant strain UTI89Δ*csgA*; and (iii) the complete extracellular matrix (ECM). These spectra indicated that the biofilm matrix formed by curli-producing bacteria has two major components, curli and cellulose, each in a quantifiable amount. The curli-only spectra were obtained from native curli prepared from the strain MC4100 that only produces curli at the cell surface. Curli were obtained using our optimized protocol to isolate curli fibers through shear homogenization, avoiding cell lysis, with subsequent SDS washing and centrifugation, tracked by protein gel and western blot characterization. Protein gel analysis was performed with and without formic acid treatment, as is typical for amyloids, where formic acid treatment is required to disassemble curli for migrating through a polyacrylamide gel. The one-dimensional curli natural-abundance ^{13}C NMR spectrum naturally contained contributions from all of the CsgA residues, including a notable downfield shoulder in the carbonyl peak that is consistent with the high propensity of Gln and Asn residues, with their carbonyl-containing sidechains, in the CsgA subunit [18]. The cellulose material was isolated from the biofilm-forming strain, UTI89, lacking the *csgA* gene: UTI89Δ*csgA*. This material was certain to lack curli, but would contain cellulose and possibly other components. As mentioned in the previous section, the material contained flagella prior to SDS washing, but not as an intimate part of the insoluble network and matrix and is dispensable for UTI89 biofilm formation on agar. By NMR, the SDS-washed cellulose material produced by UTI89Δ*csgA* appeared to be a modified form of a cellulose, where CPMAS and Rotational-Echo Double-Resonance (REDOR) [32] NMR spectra suggested the presence of an aminoethyl modification to the polysaccharide. There were no other protein or unrelated chemical shifts associated with this sample, which together with the protein characterization, indicated that the overall bottom-up analysis would be simpler than we anticipated. We discovered that a spectral sum of the two samples (pure curli and the extracellular material from the curli mutant, UTI89Δ*csgA*) was able to completely recapitulate the CPMAS spectrum of the wild-type UTI89 ECM (Fig. 1). Thus, from the spectral scaling we determined that the ECM was composed of only two major components by mass: curli amyloid fibers (85%) and a modified form of cellulose (15%). An additional sample that contained a physical mixture of the two major parts combined in the 6:1 ratio in one sample rotor additionally confirmed the compositional determination [18]. This was the first quantification of the components of the intact ECM from a bacterial biofilm.

In addition, we have reported NMR spectra for intact bacterial biofilms, including *cells plus the ECM*, that have been valuable for comparing the total carbon pools of biofilms formed under different conditions [9,30], although very selective assignments are more challenging in whole-biofilm samples. What should be emphasized here is that the bottom-up approach introduced in our *E. coli* ECM study was made possible by having samples corresponding to separate biofilm parts. By collecting the ^{13}C NMR

spectra of known biofilm parts, one can determine how well they account for the total compositional profile from the intact biofilm matrix with all the parts present. This bottom-up approach should also be applicable to other macromolecular and whole-cell assemblies.

3. Extracellular matrix composition of *V. cholerae* agar biofilms: a top-down NMR approach

3.1. A more complex matrix

The approach employed above for *E. coli* is appropriate when separate samples of major biofilm parts are available or can be approximated by available NMR spectra of related components. In our second major study of the composition of the bacterial extracellular matrix, we examined biofilms formed by *V. cholerae*, the causative agent of cholera, noting that we worked with the cholera toxin mutant that is unable to cause disease. Several proteins, including Bap1, RbmA, and RbmC, as well as the complex Vibrio exopolysaccharide, also known as VPS, have been identified as being present in the extracellular matrix [33–36], but with no estimation of the extent to which each is present in the material. Outer membrane vesicles comprised of lipopolysaccharides have also been detected in *V. cholerae* biofilms [37–39]. Together these provide a starting "parts list" for the *V. cholerae* ECM.

3.2. The top-down approach

A similar approach to that described above could be taken and would require optimization of the separate polysaccharide and single protein expression and production systems to generate sufficient quantities of the candidate matrix parts for NMR analysis. However, we took the opportunity to develop a new top-down methodology to extract quantitative atomic-level parameters from this ECM system [19], appreciating it would be much more complex than the *E. coli* matrix composition described above. This approach can be applied to the many biofilms for which there is much less information available regarding potential biofilm parts, with only the complex matrix material to dissect biochemically and spectroscopically.

In our top-down approach, carbon and nitrogen NMR spectra of a uniformly ^{15}N-labeled *V. cholerae* extracellular matrix sample provide an overall compositional profiling, while recoupling measurements, specifically ^{13}C{^{15}N}, ^{13}C{^{31}P}, and ^{15}N{^{31}P} REDOR measurements, allowed for enhanced annotation and quantification of the carbon and nitrogen pools. The ECM sample in this case was prepared from *V. cholerae* grown on a minimal agar medium. ECM was extracted by simple overnight rocking in 50-mL conical tubes, which for *V. cholerae* was sufficient to remove ECM from the cells. After cell removal by low-speed centrifugation, the ECM material in the supernatant was dialyzed against water, frozen, and lyophilized.

3.3. First-level accounting of general carbon types from CPMAS

The first inspection of the ^{13}C CPMAS spectrum immediately revealed that the *V. cholerae* ECM was polysaccharide rich with significant carbon intensity in the 60–100 ppm range (Fig. 2). Carbon chemical shifts were also observed that were consistent with proteins (carbonyl, 171 ppm; α-carbons, 51–58 ppm; other aliphatics 10–40 ppm), glycine (α-carbons, 38–43 ppm), acetyl modifications (20–22 ppm), lipids (20, 28, and 171 ppm), and possibly DNA. To use the CPMAS peak areas quantitatively, one must account for the possible influence of differences in cross polarization of different spin types. Thus, CPMAS was performed as a function of CP time and CP buildup curves were provided for each distinguishable peak in the spectrum, where extrapolations to time zero from data at long CP times provide normalized intensities. Except for the sharp lipid-like peak at 28 ppm, the CP behavior of the other carbons was similar with little or no change to the relative integrated carbon contributions, suggesting that they experience a similar overall proton spin system. In our experience, many of our intact whole-cell and cell-wall samples behave this way, for lyophilized solids with NMR measurements performed on 200–500 MHz spectrometers with modest spinning speeds (under 8 kHz).

The anomeric and complementary sugar-ring carbons have unique carbon chemical shifts and provided the start of the carbon accounting. 8.5% of all the carbon intensity in the spectrum was attributed to the anomerics while 34% was due to the other sugar ring carbons. It was reassuring to obtain this experimental 4:1 integrated ratio for non-anomeric sugar carbons to anomeric carbons as expected for a sugar ring system. Thus, we knew that 43% of the total carbons arise from collective sugar ring carbons. We anticipated that the overall polysaccharide carbon contribution would be even larger as studies on isolated polysaccharide parts have revealed that *V. cholerae* polysaccharides are highly modified.

3.4. Detailed carbon accounting of the V. cholerae ECM using REDOR as a spectroscopic ruler and filter to identify and quantify one-bond C–N pairs and longer range C–P couplings

Given the redundancy among other chemical shifts, ^{13}C{^{15}N} REDOR permitted further specification. Carbons were present at natural abundance and we employed ^{13}C{^{15}N}REDOR to select for one-bond C–N couplings. Although REDOR is typically recognized for its ability to obtain long-range distance information through the accurate determination of heteronuclear dipolar couplings, we often use REDOR as a spectroscopic filter as described here to dissect spectra of complex systems. One-bond ^{13}C{^{15}N}REDOR (REDOR evolution time of 1.68 ms) provided an upper limit on the percent of carbons that could be assigned to alpha carbons in contrast to other carbons that could contribute to peak intensity between 40 and 60 ppm that are not directly bonded to a nitrogen. We determined that the upper limit on alpha carbons (for all amino acids except glycine) was 6%. Accompanying this was the estimate of glycine alpha carbons as contributing to 4% of the carbon pool, which would be surprising given that glycine is one of twenty amino acids. Although glycine can be more prevalent than many amino acids in proteins, one would not expect this contribution to be more than about 10% of the alpha carbons, or about 0.6% of the total carbon pool. The structure of an isolated soluble polysaccharide unit has been reported, however, and has a complex structure, with N-acetyl, O-acetyl, and glycine modifications on a single sugar ring. Thus, the results indicated that many of the sugars may be accompanied by a glycine modification. Given that approximately 9% of the carbons are anomerics and about 3% of the glycine carbons are likely involved in modifications, up to one-third of the polysaccharides may be modified with glycine. The carbonyl intensity also indicated that carbonyls contribute to 16% of the carbon mass, where only 75% of those were directly bonded to a nitrogen as determined by REDOR. Thus, a maximum of 12% of the carbon was assigned to peptides and sugar N-acetyl modifications, providing an additional parameter in accounting for the ECM carbon. About 10% of the ECM carbonyls would be expected to be associated with their respective alpha carbons (6% non-Gly and 4% Gly described above), leaving about 2% for carbonyls with an adjacent nitrogen in polysaccharide modifications, such as with N-acetyl groups. The remaining 4% of carbonyls not directly bonded to ^{15}N could arise from lipid headgroups, Asp and Glu sidechains, and glycine modifications on polysaccharides. The presence of lipids was also confirmed by ^{13}C{^{31}P}REDOR

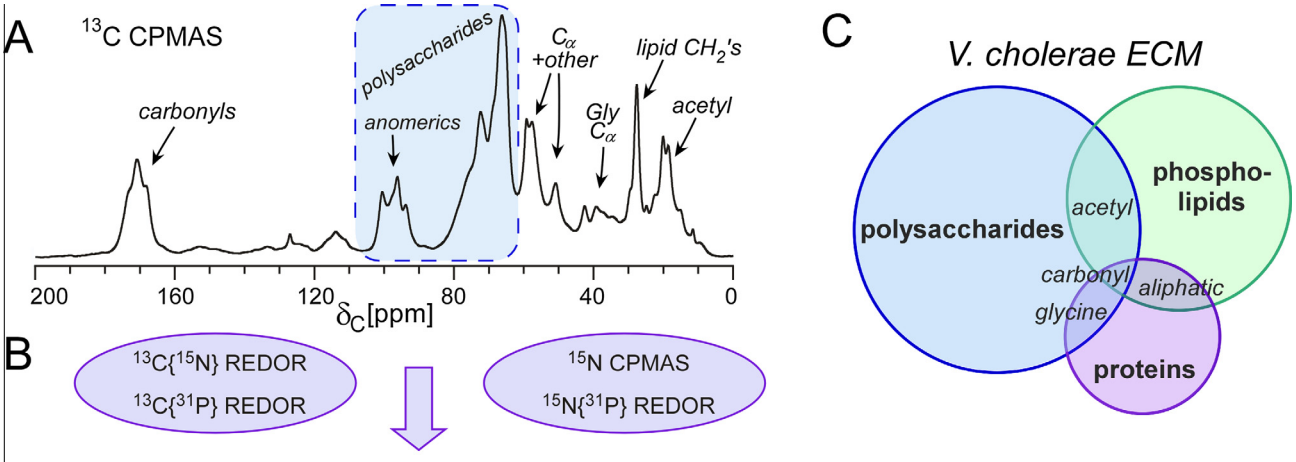

Defined carbon pools in *V. cholerae* ECM (minimal agar media)

Chemical Shift, C_{13}	171 ppm	94-100 ppm	60-80 ppm	50-60 ppm	38-43 ppm	25-30 ppm	10-25 ppm
Carbon type	carbonyls	anomerics	ring carbons	other C_α	Gly C_α	CH_2's	C-x-N aliphatics
Carbon mass (% of total)	16%	9%	34%*	6%	4%	6%	7%
Molecules	amino acids, phospholipids, N- and O-acetyl modifications	sugars	sugars	amino acids	Gly	phospholipids, amino acids	amino acids, acetyl modifications

Representative Chemical Structures

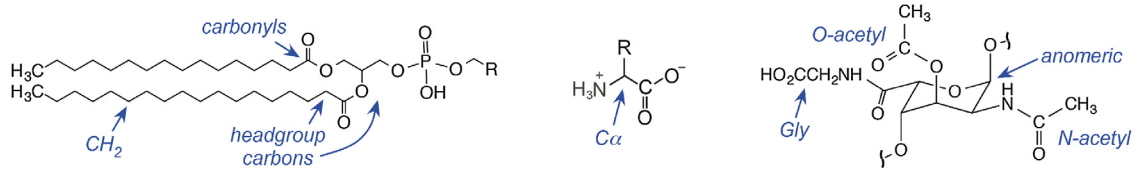

Fig. 2. The top-down approach: *V. cholerae* ECM composition by solid-state NMR. (A) The ^{13}C CPMAS spectrum indicates that the ECM is polysaccharide rich and provides a snapshot of all of the general carbon types in the ECM. (B) REDOR experiments allowed for spectral editing and quantitation of more specific carbon pools as summarized in the table accompanied by illustrated molecular components and their carbon contributions. (C) Graphical summary of approximate *V. cholerae* ECM compositional pools. This figure is adapted from Ref. [19].

performed at a longer evolution time of 8.95 ms to monitor the carbonyls and nearby carbons proximate to ^{31}P in lipid headgroup regions, where the REDOR difference spectrum was comparable to ^{13}C{^{31}P} REDOR spectra of a pure lipid sample. The remaining spectral contributions in the aliphatic region were also consistent with the defined contributions described above and together provided a total accounting of the types of carbons and estimation of the carbon content in polysaccharide, lipid, and protein pools (Fig. 2).

Given the several candidates for possible proteins in the ECM, we did not uniquely quantify the amount of distinct proteins, but rather accounted for the types of molecular carbon present in the ECM, a valuable approach in such a complex ECM-perhaps one of the most complex we will encounter. Protein gels were also obtained of the ECM material [19] and standard mass mapping with mass spectrometry or N-terminal sequencing can identify those proteins and help to assess specific protein contributions that can be compared across samples when the proteins are soluble or can be solubilized well and run into a protein gel. Future comparisons with reference samples of individual polysaccharide, lipid, and proteins contributions can also be made in the spirit of the *E. coli* approach described above. Yet, while important genetic and molecular determinants have been identified for *V. cholerae* biofilm formation, our solid-state NMR approach provided crucial parameters to place the key types of molecular players into the greater compositional context of the intact *V. cholerae* ECM.

4. Conclusions and future avenues

We have developed new approaches that help to transform vague biofilm descriptors from terms like "glue" and "slime" into quantitative parameters of chemical and molecular composition. In our work with amyloid-integrated *E. coli* biofilms, we provided the first quantitative determination of the composition of the intact extracellular matrix of a bacterial biofilm. In this "sum-of-the-parts" bottom-up approach, ^{13}C NMR spectra of separate matrix components were able to completely recapitulate the spectrum of the intact ECM. In our work with the more complex *V.*

cholerae biofilms, we developed an alternative top-down NMR approach that only required the intact ECM material and did not rely on samples corresponding to isolated matrix components. With these two examples so far, we find that bacteria can employ very different matrix-assembly strategies to build an ECM that provides protection to the bacterial community. In the case of *E. coli* biofilms grown on YESCA agar, the ECM is protein-rich and in the case of *V. cholerae*, the compositional balance of the ECM is more polysaccharide-rich, with lipids and proteins helping to contribute to an overall more complex ECM. Most biofilm studies and reviews have emphasized the prominent role that polysaccharides play in biofilm communities and our determination that the *E. coli* ECM contained much more protein than polysaccharide was a surprise. It may be that amyloid fibers are unique among proteins for their ability to contribute to aggregation and structural matrix assembly. We have suggested that the presence of hydrophobic proteins, in general, may be necessary for biofilm formation at air–liquid interfaces [29] and the same may also apply to biofilms on solid surfaces such as agar and plastic. Future work examining other amyloid-integrated biofilms and non-amyloid-associated biofilms are needed to explore these possibilities.

To summarize the immediate and evolving impact of our analytical developments in characterizing matrix composition, the solid-state NMR approaches we have introduced for compositional analysis of biofilm matrices are not subject to sampling bias or destruction of matrix material that is required of most analyses employed to characterize the composition of ECM material. One must fully describe and characterize the type of sample being investigated and how the ECM was prepared, with characterization by at least microscopy and protein gel analysis, and different isolation protocols may be suited to different biofilms. The NMR spectra then report on the total accounting of NMR-active nuclei in a given sample. We have examined ^{13}C, ^{15}N, and ^{31}P pools in our biofilm work. Both bottom-up and top-down approaches involve a panel of one-dimensional NMR experiments that can be employed on any spectrometer equipped to perform solid-state NMR measurements, where the REDOR measurements require a three-channel probe and spectrometer.

Future avenues for the *E. coli* biofilms described here involve the integration of higher resolution microscopy to improve our understanding of the spatial arrangements of matrix parts and polymers in the ECM. Indeed, super-resolution imaging of *V. cholerae* biofilms was important for visualizing and locating specific proteins within the intact biofilm and proposing distinct roles regarding cell-surface adhesion and cell–cell adhesion, for example [40]. Similar visualization will be invaluable in understanding the spatial arrangements of curli and cellulose in the amyloid-integrated *E. coli* biofilms. We are also working to measure the atomic-level proximities between matrix components in the *E. coli* ECM by NMR. Parameters of biofilm architecture will further refine our developing description of a biofilm and its corresponding ECM as an organized assembly of polymeric macromolecules, connecting composition, architecture, and function. Toward these goals of detailing ECM architecture, there are exciting opportunities to recruit creative NMR detection schemes, coupled to traditional or new biosynthetic labeling strategies to build from the foundation provided by the compositional determinations described in this perspective. Determinations of matrix architecture will also be invaluable in helping to determine the modes of action of biofilm inhibitors, particularly ones that may prevent proper matrix assembly.

Acknowledgments

Electron microscopy images in Fig. 1B and C were kindly provided by Dr. Ji Youn Lim, and assistance from the Stanford Cell Sciences Imaging Facility is acknowledged. L.C. gratefully acknowledges support from the NIH Director's New Innovator Award, Stanford University, and the Stanford Terman Fellowship.

References

[1] F. Bloch, W.W. Hansen, M. Packard, The nuclear induction experiment, Phys. Rev. 70 (1946) 474–485.
[2] E.M. Purcell, H.C. Torrey, R.V. Pound, Resonance absorption by nuclear magnetic moments in a solid, Phys. Rev. 69 (1946) 37–38.
[3] J.C. Kendrew, R.E. Dickerson, B.E. Strandberg, R.G. Hart, D.R. Davies, D.C. Phillips, V.C. Shore, Structure of myoglobin – 3-dimensional Fourier synthesis at 2 a resolution, Nature 185 (1960) 422–427.
[4] M.F. Perutz, M.G. Rossmann, A.F. Cullis, H. Muirhead, G. Will, A.C.T. North, Structure of haemoglobin – 3-dimensional Fourier synthesis at 5.5-a resolution, obtained by X-ray analysis, Nature 185 (1960) 416–422.
[5] L. Hall-Stoodley, J.W. Costerton, P. Stoodley, Bacterial biofilms: from the natural environment to infectious diseases, Nat. Rev. Microbiol. 2 (2004) 95–108.
[6] R.M. Donlan, J.W. Costerton, Biofilms: survival mechanisms of clinically relevant microorganisms, Clin. Microbiol. Rev. 15 (2002). 167-+..
[7] J.W. Costerton, P.S. Stewart, E.P. Greenberg, Bacterial biofilms: a common cause of persistent infections, Science 284 (1999) 1318–1322.
[8] P. Watnick, R. Kolter, Biofilm, city of microbes, J. Bacteriol. 182 (2000) 2675–2679.
[9] C. Reichhardt, L. Cegelski, Solid-state NMR for bacterial biofilms, Mol. Phys. 112 (2014) 887–894.
[10] H.C. Flemming, J. Wingender, The biofilm matrix, Nat. Rev. Microbiol. 8 (2010) 623–633.
[11] B. Zhang, R. Powers, Analysis of bacterial biofilms using NMR-based metabolomics (vol. 4, pg. 1273, 2012), Future Med. Chem. 4 (2012). 1764-1764.
[12] J. Fang, P.C. Dorrestein, Emerging mass spectrometry techniques for the direct analysis of microbial colonies, Curr. Opin. Microbiol. 19 (2014) 120–129.
[13] J.D. Watrous, P.C. Dorrestein, Imaging mass spectrometry in microbiology, Nat. Rev. Microbiol. 9 (2011) 683–694.
[14] I.W. Sutherland, Biofilm exopolysaccharides: a strong and sticky framework, Microbiol. – Uk 147 (2001) 3–9.
[15] D.G. Allison, The biofilm matrix, Biofouling 19 (2003) 139–150.
[16] E. Karunakaran, J. Mukherjee, B. Ramalingam, C.A. Biggs, "Biofilmology": a multidisciplinary review of the study of microbial biofilms, Appl. Microbiol. Biot. 90 (2011) 1869–1881.
[17] Y.Q. Jiao, G.D. Cody, A.K. Harding, P. Wilmes, M. Schrenk, K.E. Wheeler, J.F. Banfield, M.P. Thelen, Characterization of extracellular polymeric substances from acidophilic microbial biofilms, Appl. Environ. Microb. 76 (2010) 2916–2922.
[18] O.A. McCrate, X.X. Zhou, C. Reichhardt, L. Cegelski, Sum of the parts: composition and architecture of the bacterial extracellular matrix, J. Mol. Biol. 425 (2013) 4286–4294.
[19] C. Reichhardt, J.C.N. Fong, F. Yildiz, L. Cegelski, Characterization of the *Vibrio cholerae* extracellular matrix: a top-down solid-state NMR approach, Biochim. et Biophys. Acta (BBA) – Biomembr. 1848 (2015) 378–383.
[20] L. Cegelski, J.S. Pinkner, N.D. Hammer, C.K. Cusumano, C.S. Hung, E. Chorell, V. Aberg, J.N. Walker, P.C. Seed, F. Almqvist, M.R. Chapman, S.J. Hultgren, Small-molecule inhibitors target *Escherichia coli* amyloid biogenesis and biofilm formation, Nat. Chem. Biol. 5 (2009) 913–919.
[21] L. Cegelski, C.L. Smith, S.J. Hultgren, Adhesion, Microbial, in: M. Schaechter (Ed.), Encyclopedia of Microbiology, third ed., Academic Press, Oxford, 2009, pp. 1–10.
[22] Y. Lim, J.S. Pinkner, L. Cegelski, Community behavior and amyloid-associated phenotypes among a panel of uropathogenic *E. coli*, Biochem. Biophys. Res. Co 443 (2014) 345–350.
[23] A. Olsen, A. Jonsson, S. Normark, Fibronectin binding mediated by a novel class of surface organelles on *Escherichia-coli*, Nature 338 (1989) 652–655.
[24] M.R. Chapman, L.S. Robinson, J.S. Pinkner, R. Roth, J. Heuser, M. Hammar, S. Normark, S.J. Hultgren, Role of *Escherichia coli* curli operons in directing amyloid fiber formation, Science 295 (2002) 851–855.
[25] U. Romling, W. Bokranz, W. Rabsch, X. Zogaj, M. Nimtz, H. Tschape, Occurrence and regulation of the multicellular morphotype in Salmonella serovars important in human disease, Int. J. Med. Microbiol. 293 (2003) 273–285.
[26] C. Beloin, A. Roux, J.M. Ghigo, *Escherichia coli* biofilms, Curr. Top Microbiol. 322 (2008) 249–289.
[27] C. Wu, J.Y. Lim, G.G. Fuller, L. Cegelski, Quantitative analysis of amyloid-integrated biofilms formed by uropathogenic *Escherichia coli* at the air–liquid interface, Biophys. J. 103 (2012) 464–471.
[28] C. Wu, J.Y. Lim, G.G. Fuller, L. Cegelski, Disruption of *Escherichia coli* amyloid-integrated biofilm formation at the air–liquid interface by a polysorbate surfactant, Langmuir 29 (2013) 920–926.
[29] Emily C. Hollenbeck, Jiunn C.N. Fong, Ji Y. Lim, Fitnat H. Yildiz, Gerald G. Fuller, L. Cegelski, Molecular determinants of mechanical properties of *V. cholerae* biofilms at the air–liquid interface, Biophys. J. 107 (2014) 2245–2252.
[30] J.Y. Lim, J.M. May, L. Cegelski, Dimethyl sulfoxide and ethanol elicit increased amyloid biogenesis and amyloid-integrated biofilm formation in *Escherichia coli*, Appl. Environ. Microb. 78 (2012) 3369–3378.
[31] X. Zogaj, M. Nimtz, M. Rohde, W. Bokranz, U. Romling, The multicellular morphotypes of Salmonella typhimurium and *Escherichia coli* produce

cellulose as the second component of the extracellular matrix, Mol. Microbiol. 39 (2001) 1452–1463.
[32] T. Gullion, J. Schaefer, Rotational-echo double-resonance NMR, J. Magn. Reson. 81 (1989) 196–200.
[33] F.H. Yildiz, G.K. Schoolnik, *Vibrio cholerae* O1 El Tor: identification of a gene cluster required for the rugose colony type, exopolysaccharide production, chlorine resistance, and biofilm formation, Proc. Natl. Acad. Sci. USA 96 (1999) 4028–4033.
[34] J.C.N. Fong, K. Karplus, G.K. Schoolnik, F.H. Yildiz, Identification and characterization of RbmA, a novel protein required for the development of rugose colony morphology and biofilm structure in *Vibrio cholerae*, J. Bacteriol. 188 (2006) 1049–1059.
[35] J.C.N. Fong, F.H. Yildiz, The rbmBCDEF gene cluster modulates development of rugose colony morphology and biofilm formation in *Vibrio cholerae*, J. Bacteriol. 189 (2007) 2319–2330.
[36] J.C.N. Fong, K.A. Syed, K.E. Klose, F.H. Yildiz, Role of Vibrio polysaccharide (vps) genes in VPS production, biofilm formation and *Vibrio cholerae* pathogenesis, Microbiol. – Sgm 156 (2010) 2757–2769.
[37] M. Duperthuy, A.E. Sjostrom, D. Sabharwal, F. Damghani, B.E. Uhlin, S.N. Wai, Role of the *Vibrio cholerae* matrix protein bap1 in cross-resistance to antimicrobial peptides, PLOS Pathog. 9 (2013).
[38] E. Altindis, Y. Fu, J.J. Mekalanos, Proteomic analysis of *Vibrio cholerae* outer membrane vesicles, Proc. Natl. Acad. Sci. USA 111 (2014) E1548–E1556.
[39] D.R. Leitner, S. Feichter, K. Schild-Prufert, G.N. Rechberger, J. Reidl, S. Schild, Lipopolysaccharide modifications of a cholera vaccine candidate based on outer membrane vesicles reduce endotoxicity and reveal the major protective antigen, Infect. Immun. 81 (2013) 2379–2393.
[40] V. Berk, J.C.N. Fong, G.T. Dempsey, O.N. Develioglu, X.W. Zhuang, J. Liphardt, F.H. Yildiz, S. Chu, Molecular architecture and assembly principles of *Vibrio cholerae* biofilms, Science 337 (2012) 236–239.